Static groundwater levels were corrected for tidal influence following the procedures discussed in Section 5.4.1. Mean groundwater elevations for the upper aquifer zone were calculated using the upper screen of NoVOCs™ well and the three upper zone NoVOCs™ observation wells (MW-45, MW-48, and MW-52). Mean groundwater elevations for the lower aquifer zone were calculated using the three lower zone NoVOCs™ observation wells (MW-47, MW-49, and MW-53). The mean groundwater elevations after tidal correction are listed in Table 5-8.

The equivalent fresh-water heads of the mean groundwater elevations were calculated following the procedures discussed in Section 5.4.2. The first step of the calculation is to obtain density data for various monitoring well locations and aquifer depths because the groundwater density was not directly measured. Jacobs Engineering Group, Inc. (1995b) applied an empirical equation developed by de Marsily (1986) to calculate groundwater density from total dissolved solids (TDS) data. The empirical equation was developed based on a laboratory test with sodium chloride solution and a linear regression analysis.

The empirical equation developed by de Marsily (1986) is as follows:

$$r = \left( 6.87 \times 10^{-4} \, C_{TDS} \right) + 998.4575 \qquad (5\text{-}42)$$

where

| | | |
|---|---|---|
| $\rho$ | = | Groundwater density (kg/m$^3$) |
| $C_{TDS}$ | = | TDS concentration (mg/L) |

The groundwater density and results for equivalent fresh-water head calculation are presented in Table 5-8.

The mean equivalent fresh-water head contours for the upper aquifer zone are plotted in Figures 5-33 and 5-34. Figure 5-33 is based on four points (including data for well MW-48), and Figure 5-34 is based on three points (excluding data for well MW-48). The two presentations (with and without data for well MW-48 data) are provided because the screen of well MW-48 is at a lower elevation than in the other three wells used to construct the contours. The mean equivalent fresh-water head contours for the lower aquifer zone are plotted in Figure 5-35. These contour maps represent the mean static water levels and flow directions with tidal and pumping influences removed. Effects caused by variation in groundwater

density variation were also corrected. These contour maps are considered representative of the natural groundwater flow pattern.

As shown in Figures 5-33, 5-34, and 5-35, groundwater generally flows to the west or northwest in both of the upper and lower aquifer zones. The horizontal hydraulic gradient in both aquifer zones is relatively flat, ranging from 0.005 to 0.01 feet per feet in the upper zone and approximately 0.006 in the lower zone. Data for generating the contour maps were limited (four points for the upper aquifer zone and three points for the lower aquifer zone) because other NoVOCs™ observation wells were completed at depths between the two aquifer zones. Also, data were not available for some of the observation wells because of data logger malfunction.

### 5.4.4 Vertical Hydraulic Gradient Correction

Calculation of vertical hydraulic gradient in a fresh-water aquifer (groundwater density of 1 $g/cm^3$) is simple: for two vertically aligned wells, the vertical hydraulic gradient equals the head difference between the wells divided by the distance between the midpoint of the well screen intervals. However, calculation of vertical hydraulic gradient in a density-variable aquifer is relatively complex. Incorrect calculations of the vertical hydraulic gradient by simply using equivalent fresh-water heads to determine the head difference are common. The vertical hydraulic gradient in a density-variable aquifer is a function of the equivalent fresh-water heads, the distance between the two intervals, and the groundwater density. This section discusses the principles and the reason for calculating vertical hydraulic gradient differently from the horizontal hydraulic gradient. The procedures to calculate the vertical hydraulic gradient in a density-variable aquifer are also presented.

Vertical hydraulic gradient is not calculated in this report because limited groundwater density data are available. Also, vertical hydraulic gradient was not identified as a key parameter in the pumping test data analysis and NoVOCs™ well evaluation. The equations and procedures discussed in this section can be followed in future data analysis for the vertical hydraulic gradient at the site.

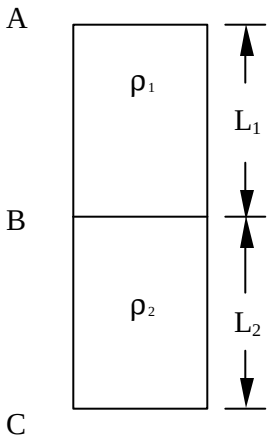


Considering water column ABC filled with a porous medium as shown in the Drawing: the upper portion, AB, has a height $L_1$ and contains water (or any fluid) with a density equal to $\rho_1$; the lower portion, BC, has a height of $L_2$ and contains water with a density equal to $\rho_2$. Water in the column is assumed to be in a hydraulic steady state, that is, no vertical flow occurs. Vertical hydraulic gradient is to zero between any two points within the column. Also, it is assumed that no density-driven flow and no density diffusion occur across the boundary line B.

If the bottom of the column is set at the datum, that is, the elevation z equals zero at point C, from Equation 5-39, the equivalent fresh water-head at the three points (A, B, and C) will be given as:

$$h_A^* = z_A + \frac{p_A}{r_0 g} \qquad (5\text{-}43)$$

$$h_B^* = z_B + \frac{p_B}{r_0 g} \qquad (5\text{-}44)$$

$$h_C^* = z_C + \frac{p_C}{r_0 g} \qquad (5\text{-}45)$$

where

$p_A$, $p_B$, and $p_C$ = The groundwater pressure gages at points A, B, and C

$z_A$, $z_B$, and $z_C$ = The elevations of points A, B, and C

Equations 5-43, 5-44, and 5-45 can be solved as follows, considering $p_A=0$, $p_B=\rho_1 g L_1$, $p_C=\rho_1 g L_1+\rho_2 g L_2$, $z_A=L_1+L_2$, $z_B=L_2$, and $z_C=0$:

$$h_A^* = (L_1 + L_2) + 0 = L_1 + L_2 \qquad (5\text{-}46)$$

$$h_B^* = L_2 + \frac{r_1 g L_1}{r_0 g} = g_1 L_1 + L_2 \qquad (5\text{-}47)$$

$$h_C^* = 0 + \frac{(r_1 L_1 + r_2 L_2) g}{r_0 g} = g_1 L_1 + g_2 L_2 \qquad (5\text{-}48)$$

Because $\gamma_1 \neq \gamma_2 \neq 1$, Equation 5-46, 5-47, and 5-48 show that the equivalent fresh-water heads at the three points are not equal. This result contradicts the assumption that no vertical flow occurs in the water column. Therefore, the difference in the two equivalent fresh-water heads divided by the distance between the two points does not equal the vertical hydraulic gradient in aquifers with variable density groundwater.

In general, the vertical hydraulic gradient between two vertically aligned points within variable density groundwater equals the difference of the fresh-water equivalent heads at the two points divided by the distance plus a constant. That is:

$$I_{AB} = \frac{h_A^* - h_B^*}{L_1} + C_1 \qquad (5\text{-}49)$$

$$I_{BC} = \frac{h_B^* - h_C^*}{L_2} + C_2 \qquad (5\text{-}50)$$

$$I_{AC} = \frac{h_A^* - h_C^*}{L_1 + L_2} + C_3 \qquad (5\text{-}51)$$

where

$I_{AB}$ = Vertical hydraulic gradient between points A and B.

$I_{BC}$ = Vertical hydraulic gradient between points B and C.

$I_{AC}$ = Vertical hydraulic gradient between points A and C.

From Equations 5-46, 5-47, and 5-48, considering $I_{AB} = I_{BC} = I_{AC} = 0$, for steady state condition, we can solve $C_1$, $C_2$ and $C_3$ as:

$$C_1 = \frac{h_B^* - h_A^*}{L_1} = \frac{g_1 L_1 + L_2 - (L_1 + L_2)}{L_1} = g_1 - 1 \quad (5\text{-}52)$$

$$C_2 = \frac{h_C^* - h_B^*}{L_2} = \frac{g_1 L_1 + g_2 L_2 - (g_1 L_1 + L_2)}{L_2} = g_2 - 1 \quad (5\text{-}53)$$

$$C_3 = \frac{h_C^* - h_A^*}{L_1 + L_2} = \frac{g_1 L_1 + g_2 L_2 - (L_1 + L_2)}{L_1 + L_2} = \frac{g_1 L_1 + g_2 L_2}{L_1 + L_2} - 1 \quad (5\text{-}54)$$

Therefore, vertical hydraulic gradient between any two points in an aquifer with density-variable groundwater can be calculated using the following general equation (based on Equations 5-49 through 5-54):

$$I_V = \frac{h_u^* - h_l^*}{l} + (g - 1) \quad (5\text{-}55)$$

where

$I_V$ = Vertical hydraulic gradient between two vertically aligned points within the aquifer (positive value represents downward gradient) [dimensionless]

$h_u$, $h_l$ = The equivalent fresh water heads at the two points (higher elevation and lower elevation points, respectively) [L]

$l$ = Vertical distance between the two points [L]

$\gamma$ = Specific gravity of groundwater between the two points [dimensionless]

The specific gravity of groundwater between the two points should be carefully chosen when Equation 5-55 is used. If the groundwater density is not constant between the upper and lower aquifer zones, a thickness-weighted average of the specific gravity for multiple density strata should be used. The weighted average of the specific gravity is calculated as follows:

$$g = \frac{\sum_{i=1}^{n} g_i l_i}{\sum_{i=1}^{n} l_i}, \qquad i = 1,2,\ldots n \qquad (5\text{-}56)$$

where

$\gamma$ = The weighted average of the specific gravity of groundwater

$\gamma_i$ = The specific gravity of the $i^{th}$ strata

$l_i$ = The thickness of the $i^{th}$ strata

## 5.5 DIPOLE FLOW TEST

The dipole flow test (DFT), a new single-well hydraulic test for aquifer characterization, was first proposed by Kabala (1993). The test was designed to characterize the vertical distribution of local horizontal and vertical hydraulic conductivities near the test well. Measures of the aquifer's anisotropy ratio and storativity can also be obtained through DFT data analysis. DFT is a cost-effective method for aquifer hydraulic characterization because (1) the test duration is short; the test generally lasts no more than a few hours, and (2) no investigation-derived waste is generated because the water from the pumping chamber is injected to the aquifer through recharge chamber.

### 5.5.1 Mathematical Models

Kabala (1993) presented a mathematical model describing drawdown (or water level rise) during a dipole flow test in each of the isolated chambers of a well situated in a leaky homogeneous anisotropic aquifer. Major assumptions for this original model are:

- The aquifer is homogeneous and anisotropic and horizontally situated
- The aquifer is under either leaky or confined conditions
- The test well fully penetrates the aquifer thickness
- Water is removed through one of the two open screened intervals and discharged to another interval instantaneously
- Linear vertical head distribution is assumed in the semiconfining layer (leaky aquitard)

- Water storage in the leaky aquitard is negligible
- Flows in the aquifer zones are mainly horizontal, but primarily vertical mithin the leaky aquitard
- Well bore storage and well losses are insignificant
- "Skin effect" (short-circuiting through the sand packs) is negligible

The analytical solutions for drawdown in the pumping chamber and water level rise in the recharge chamber are presented by Kabala (1993). The transient solution describing drawdown is given as follows:

$$s(t) = \frac{Q}{4pK_r b}\left\{W(u_r; b_w) + \frac{2b^2}{4p^2\Delta^2}\sum_{n=1}^{\infty}\frac{1}{n^2}[\sin\frac{np(d+2\Delta)}{b} - \sin\frac{npd}{b}]^2\, W[u_r; (b_w{}^2 + \frac{(npr_w)^2}{a^2b^2})^{1/2}]\right\} \quad (5\text{-}57)$$

where

| | | |
|---|---|---|
| s(t) | = | Drawdown in the pumping chamber [L] |
| t | = | Time since beginning of the test [L] |
| Q | = | Pumping rate [$L^3T^{-1}$] |
| $K_r$ | = | Horizontal hydraulic conductivity [$LT^{-1}$] |
| b | = | Aquifer thickness [L] |
| d | = | Distance from the top of aquifer to the top of the upper chamber [L] |
| $\Delta$ | = | Half of the length of the screen interval [L] |
| $a^2$ | = | Aquifer anisotropy ratio, defined as $K_r/K_z$ [dimensionless] |
| $W(u_r, \beta_w)$ = | | Leaky aquifer well function, defined as: |

$$W(u_r; b_w) = \int_{u_r}^{\infty}\frac{1}{y}\exp(-y - \frac{b_w{}^2}{4y})dy \quad (5\text{-}58)$$

where

| | | |
|---|---|---|
| $u_r$ | = | Dimensionless time, defined as: $r_w{}^2 S_s/4K_r t$ |
| $\beta_w$ | = | Leaky factor defined as: $r_w/(K_r bb'/K')^{1/2}$ |
| $r_w$ | = | Radius of the well casing [L] |
| $S_s$ | = | Aquifer specific storage [$L^{-1}$] |

b' = Aquitard (semi-confining layer) thickness [L]

K' = Aquitard vertical hydraulic conductivity [$LT^{-1}$]

A similar solution can be derived to describe water level rise due to injection in the recharge chamber with a negative pumping rate. Combining the pumping and injection effects, the actual drawdown in the pumping chamber is given by:

$$s(t) = \frac{Q}{pK_r b}\sum_{n=1}^{\infty}[\frac{\sin(np\Delta / b)}{np\Delta / b}]^2 \cdot \sin(np\frac{l+d}{2b})\sin(np\frac{l-d-2\Delta}{2b})\cos(np\frac{d+\Delta}{b})\cdot W[u_r;(b_w{}^2 + \frac{(npr_w)^2}{a^2b^2})^{1/2}] \qquad (5\text{-}59)$$

The solution for actual water level rise in the recharge chamber is given by:

$$s(t) = \frac{Q}{pK_r b}\sum_{n=1}^{\infty}[\frac{\sin(np\Delta / b)}{np\Delta / b}]^2 \cdot \sin(np\frac{l+d}{2b})\sin(np\frac{l-d-2\Delta}{2b})\cos(np\frac{l-\Delta}{b})\cdot W[u_r;(b_w{}^2 + \frac{(npr_w)^2}{a^2b^2})^{1/2}] \qquad (5\text{-}60)$$

Equations (5-59) and (5-60) are the transient solutions for the dipole flow test. The steady state solution for drawdown in the pumping chamber is as follows:

$$s(t) = \frac{2Q}{pK_r b}\sum_{n=1}^{\infty}[\frac{\sin(np\Delta / b)}{np\Delta / b}]^2 \cdot \sin(np\frac{l+d}{2b})\sin(np\frac{l-d-2\Delta}{2b})\cos(np\frac{d+\Delta}{b})\cdot K_0[(b_w{}^2 + \frac{(npr_w)^2}{a^2b^2})^{1/2}] \qquad (5\text{-}61)$$

Where

$K_0$ = Zero-order modified Bessel function of the second kind,

l = Distance from the top of the aquifer to the bottom of the lower screen.

### 5.5.2 Modified Dipole Flow Test Solution for Wellbore Storage

Kabala (1998) developed a new DFT model to account for wellbore storage effects in the pumping and injection chambers. In the wellbore storage DFT model, measured drawdown (or water level rise) is the

sum of aquifer drawdown and wellbore storage drawdown. Dimensionless wellbore storage parameters for the pumping and recharge chambers are defined as:

$$C_{PD} = \frac{(r_i / r_w)^2}{4S} \tag{5-62}$$

$$C_{RD} = \frac{1 - (r_i / r_w)^2}{4S} \tag{5-63}$$

where

| | | |
|---|---|---|
| $C_{PD}$ | = | Dimensionless wellbore storage parameter for the pumping chamber |
| $C_{RD}$ | = | Dimensionless wellbore storage parameter for the recharge chamber |
| $r_i$ | = | Radius of inner well casing (eductor pipe)[L] |
| $r_w$ | = | Radius of well casing [L] |
| S | = | Aquifer storativity or specific yield [dimensionless] |

Laplace transformation is used to solve the partial differential equations that describe drawdown (or water level rise) in the pumping (or recharge) chamber during the DFT where the wellbore storage effect is considered. The drawdown in the pumping chamber $s_{pump}$ can be described as:

$$s_{pump}(p) = s_{pp}(p) + s_{pi}(p) \tag{5-64}$$

where p is the Laplace transformation variable, $s_{pp}$ (p) is the drawdown caused by pumping, and $s_{pi}$ (p) is the water level caused by injection (expressed as negative drawdown). The two components of the water level response are defined as follows:

$$s_{pp}(p) = \frac{Q}{4pK_r b} \cdot \frac{\frac{2}{p} K_0(\sqrt{p}) + 4\sum_{n=1}^{\infty} \frac{a_n^{\,2}}{p} K_0(\sqrt{p + g_n^{\,2}})}{C_{PD} p^2 [\frac{2}{p} K_0(\sqrt{p}) + 4\sum_{n=1}^{\infty} \frac{a_n^{\,2}}{p} K_0(\sqrt{p + g_n^{\,2}})] + 1} \tag{5-65}$$

and

$$s_{pi}(p) = \frac{-Q}{4pK_r b}$$

$$\cdot \left\{1 - \frac{[\frac{2}{p}K_0(\sqrt{p}) + 4\sum_{n=1}^{\infty}\frac{b_n^{\,2}}{p}K_0(\sqrt{p+g_n^{\,2}})][\frac{2}{p}K_0(\sqrt{p}) + 4\sum_{n=1}^{\infty}\frac{a_n^{\,2}b_n^{\,2}}{p}K_0(\sqrt{p+g_n^{\,2}})]}{C_{RD}p^2[\frac{2}{p}K_0(\sqrt{p}) + 4\sum_{n=1}^{\infty}\frac{b_n^{\,2}}{p}K_0(\sqrt{p+g_n^{\,2}})] + 1}\right\} \quad (5\text{-}66)$$

Variables $\alpha_n$, $\beta_n$, and $\gamma_n$ are defined as follows:

$$a_n = \frac{b}{np\Delta_u} \cdot \sin(\frac{np\Delta_u}{b}) \cdot \cos[\frac{np(d+\Delta_u)}{b}] \quad (5\text{-}67)$$

$$b_n = \frac{b}{np\Delta_l} \cdot \sin(\frac{np\Delta_l}{b}) \cdot \cos[\frac{np(l-\Delta_l)}{b}] \quad (5\text{-}68)$$

$$g_n = \frac{npr_w}{b\sqrt{K_r / K_z}} \quad (5\text{-}69)$$

where:

$\Delta_u$ = Half of the upper screened interval [L]

$\Delta_l$ = Half of the lower screened interval [L]

### 5.5.3 Dipole Flow Test Data Interpretation and Aquifer Anisotropy Estimation

The dimensionless drawdown in the pumping chamber versus dimensionless time can be plotted as groups of type curves with different anisotropy ratios ($a^2 = K_r/K_z$) and storativity (or specific yield) values. The type curves are generated by plotting dimensionless drawdown $s_D$ versus dimensionless time $\tau$, which are defined as follows:

$$s_D = \frac{s(t)}{s(\infty)} \quad (5\text{-}70)$$

and

$$t = \frac{n\,t}{r_w^{\,2}} \qquad (5\text{-}71)$$

where

| | | |
|---|---|---|
| $s(\infty)$ | = | Steady state drawdown or water level rise during the DFT [L] |
| $\nu$ | = | Aquifer hydraulic diffusivity, defined as T/S or $K_r/S_s$ [$L^2T^{-1}$] |

Drawdown (or water level rise) data collected during the DFT then be normalized to dimensionless drawdown (or water level rise) with values ranging from 0 to 1, as follows:

$$s_D(t) = \frac{s(t+t_0) - s_{\min}}{s_{\max} - s_{\min}} \qquad (5\text{-}72)$$

where

| | | |
|---|---|---|
| $s_D(t)$ | = | Normalized dimensionless drawdown (or water level rise) |
| $s(t+t_0)$ | = | Drawdown (or water level rise) at time $t+t_0$ [L] |
| $t_0$ | = | The beginning time of a given step of the DFT [T] |
| $s_{max}$ | = | The maximum drawdown (or water level rise) during a given step of the DFT [L] |
| $s_{min}$ | = | The minimum drawdown (or water level rise) during a given step of the DFT [L] |

The normalized drawdown or water level rise versus time are plotted for the type curve match. A scale factor (A) is applied to the real-time plots. The scale factor is applied for two purposes: (1) transferring real time to dimensionless time so the horizontal axes of the type curves and test data are comparable, and (2) adjusting the horizontal positions of the data plots so that a best match to one of the type curves can be obtained. The scale factor is defined as:

$$A = \frac{n}{r_w^{\,2}} = \frac{K_r}{S_s r_w^{\,2}} \qquad (5\text{-}73)$$

From the type curve match, the aquifer anisotropy ratio is obtained from the value of parameter $a^2$ (which equals $K_r/K_z$). In addition, aquifer horizontal hydraulic conductivity can be calculated from the values of parameters S (or $S_y$), and A. The aquifer horizontal hydraulic conductivity K is calculated by the following equation:

$$K_r = \frac{A \cdot r_w^{\,2} S}{b} \qquad (5\text{-}74)$$

DFT data collected during Step 4 recovery in the recharge chamber were considered the most suitable for parameter estimation because the water level rise data were least affected by variations in pumping rate variations and head fluctuations.

Tidal influence during the DFT is removed using data collected from well MW-51. Comparison of water level data from the NoVOCs™ well and observation well MW-51 shows that the tidal fluctuations in the two wells are almost identical. Well MW-51 also had minimum impact from the DFT because of its distance from the NoVOCs™ well. The least-square algorithm was used to simulate the tidal fluctuations in the NoVOCs™ well. The drawdown (or water level rise) correction procedure is similar to the procedures presented in Section 5.1.

Figure 5-36 shows the recovery data plots and type curve match for the DFT Step 4 recharge chamber. The type curves are generated using the DFT model considering well bore storage. The group of the type curves in Figure 5-36 represents storativity S=0.01 and anisotropy ratios $a^2 = K_r/K_z$ = 100, 30, 10, 3, and 1. The normalized dimensionless DFT recovery data with time are represented by circles,whereas the normalized recovery data versus scaled time (dimensionless time) are plotted as thick dash line.

From the DFT recovery data plots and type curve match (Figure 5-36), the aquifer hydraulic parameters are estimated as: $K_r$ = 0.0115 cm/sec, $0.001 \leq S \leq 0.01$, and $K_r/K_z$ = 4.93. These results are very close to the parameter estimated by interpreting pumping test data (Section 5.3). The aquifer hydraulic parameters estimated through DFT are also presented in Table 5-7.

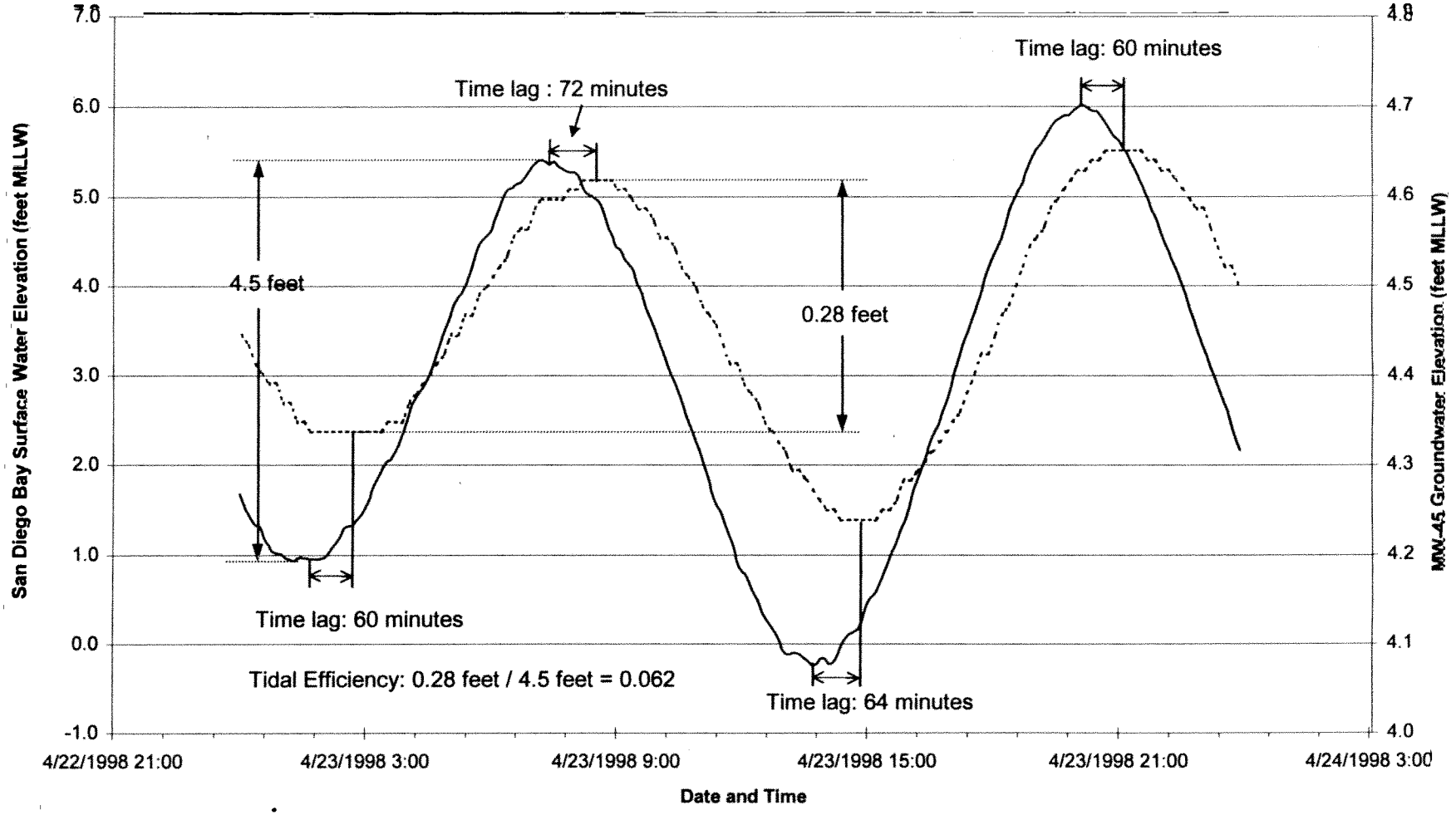


NAS NORTH ISLAND SITE 9
NoVOCs™ HYDROGEOLOGICAL INVESTIGATION

**FIGURE 5-1**
**WATER LEVEL COMPARISON BETWEEN SAN DIEGO BAY AND OBSERVATION WELL MW45**

Tetra Tech EM Inc.

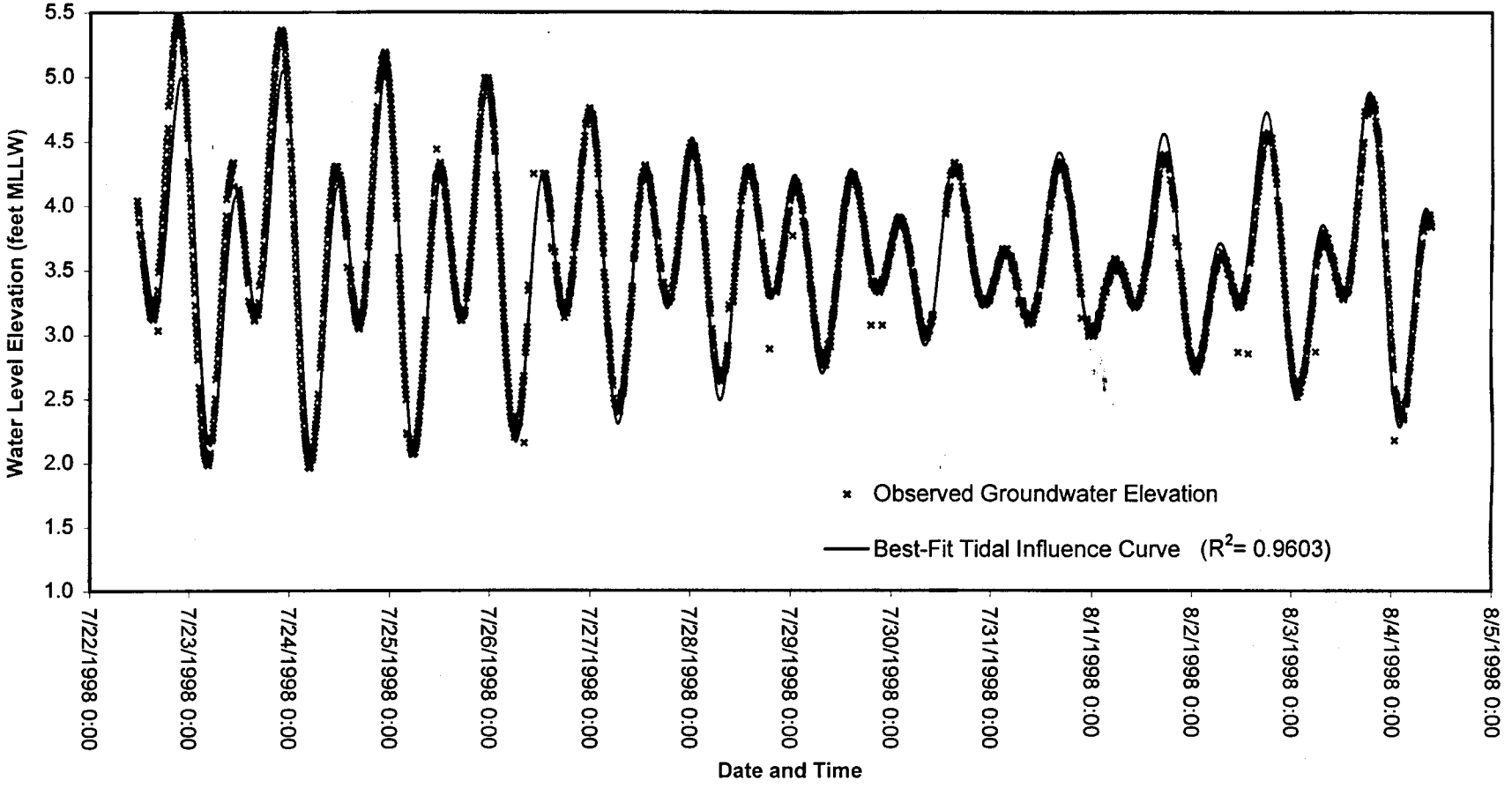


NAS NORTH ISLAND SITE 9
NoVOCs™ HYDROGEOLOGICAL INVESTIGATION

**FIGURE 5-2**
**OBSERVED GROUNDWATER ELEVATION AND BEST-FIT TIDAL INFLUENCE CURVE FOR WELL MW20**

Tetra Tech EM Inc.

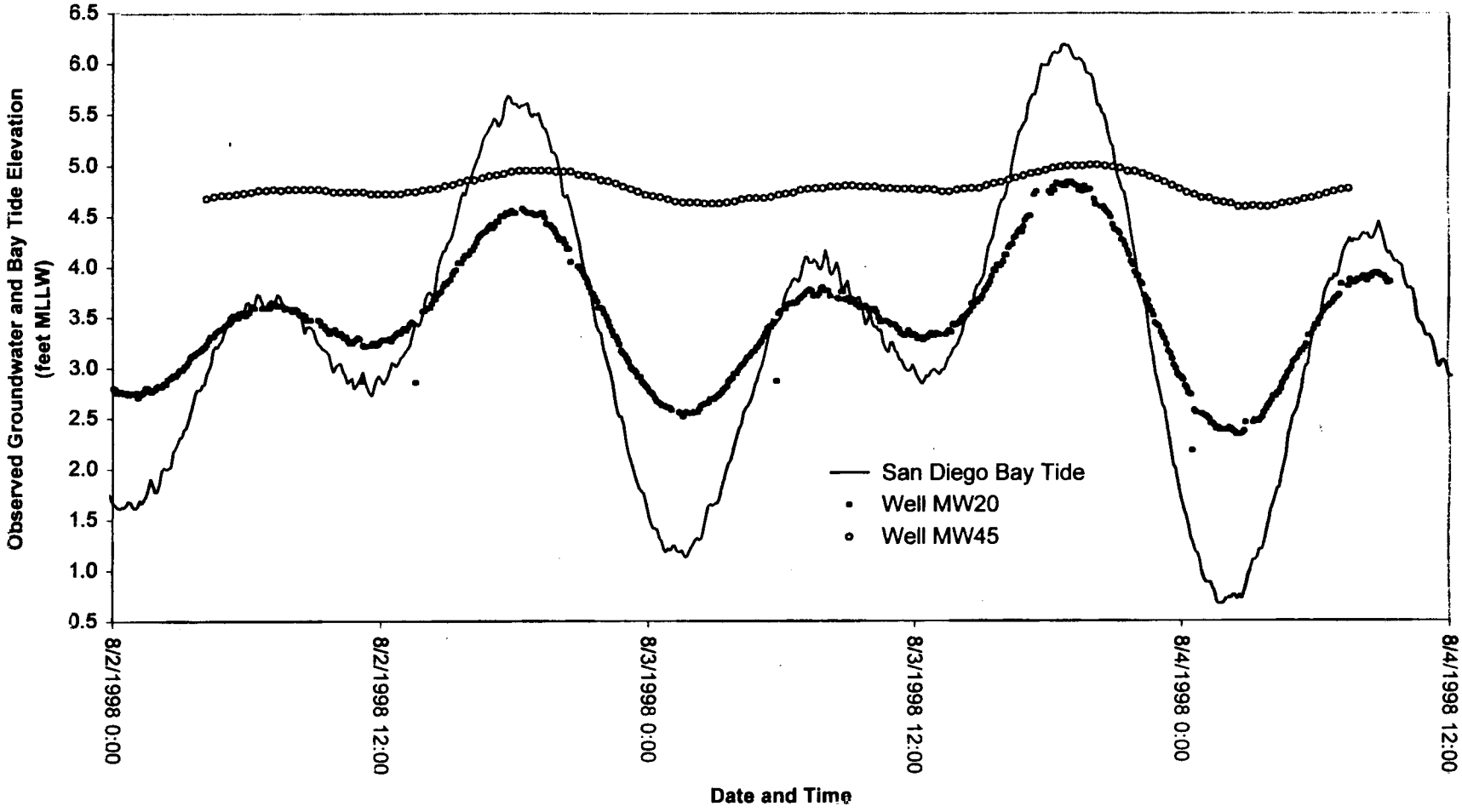


NAS NORTH ISLAND SITE 9
NoVOCs™ HYDROGEOLOGICAL INVESTIGATION

**FIGURE 5-3**
**OBSERVED WATER LEVEL COMPARISON AMONG BAY TIDE, MW20 AND MW45**

Tetra Tech EM Inc.

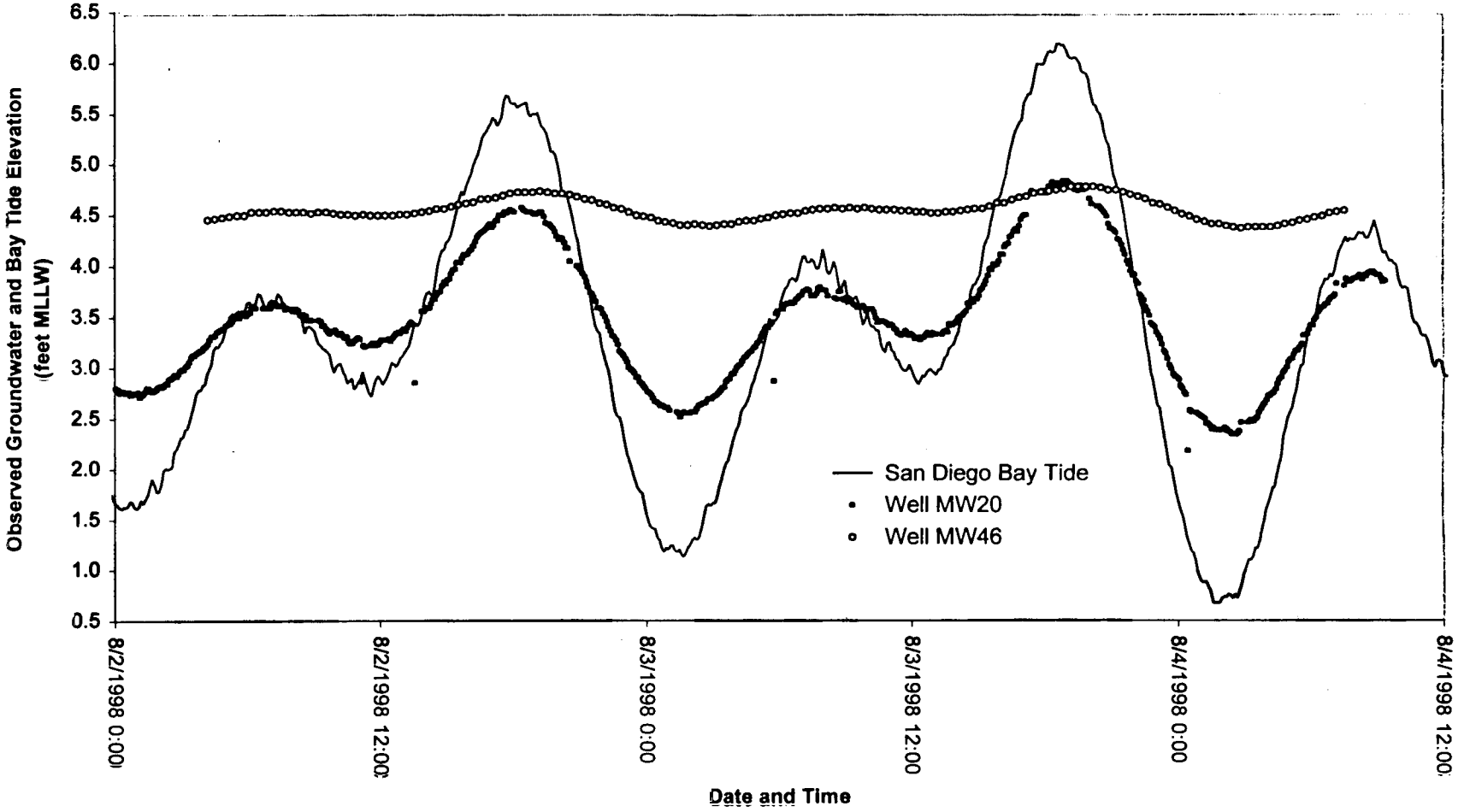


NAS NORTH ISLAND SITE 9
NoVOCs™ HYDROGEOLOGICAL INVESTIGATION

**FIGURE 5-4**
**OBSERVED WATER LEVEL COMPARISON AMONG BAY TIDE, MW20 AND MW46**

Tetra Tech EM Inc.

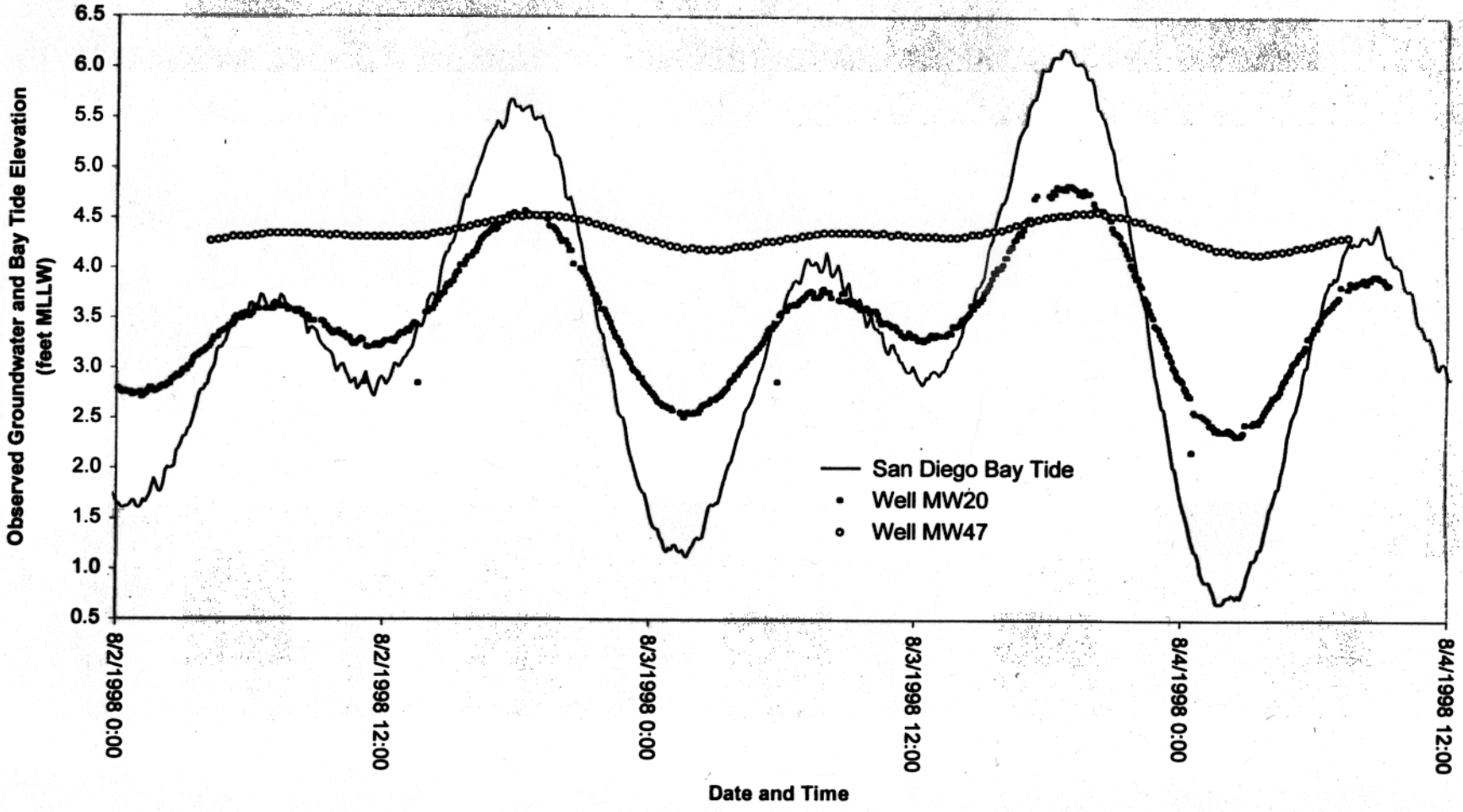


NAS NORTH ISLAND SITE 9
NoVOCs™ HYDROGEOLOGICAL INVESTIGATION

**FIGURE 5-5**
**OBSERVED WATER LEVEL COMPARISON AMONG BAY TIDE, MW20 AND MW47**

Tetra Tech EM Inc.

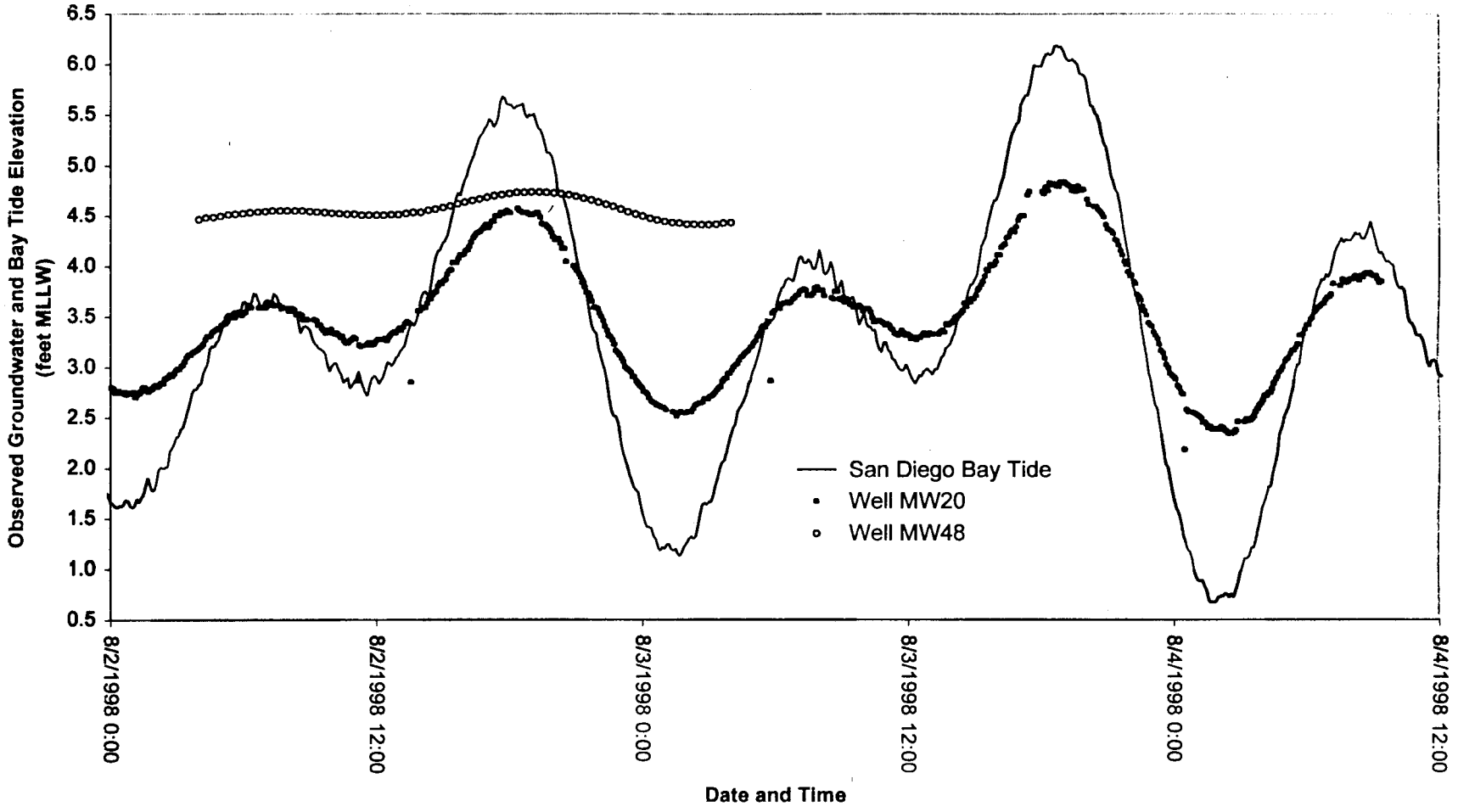


NAS NORTH ISLAND SITE 9
NoVOCs™ HYDROGEOLOGICAL INVESTIGATION

**FIGURE 5-6**
**OBSERVED WATER LEVEL COMPARISON AMONG BAY TIDE, MW20 AND MW48**

Tetra Tech EM Inc.

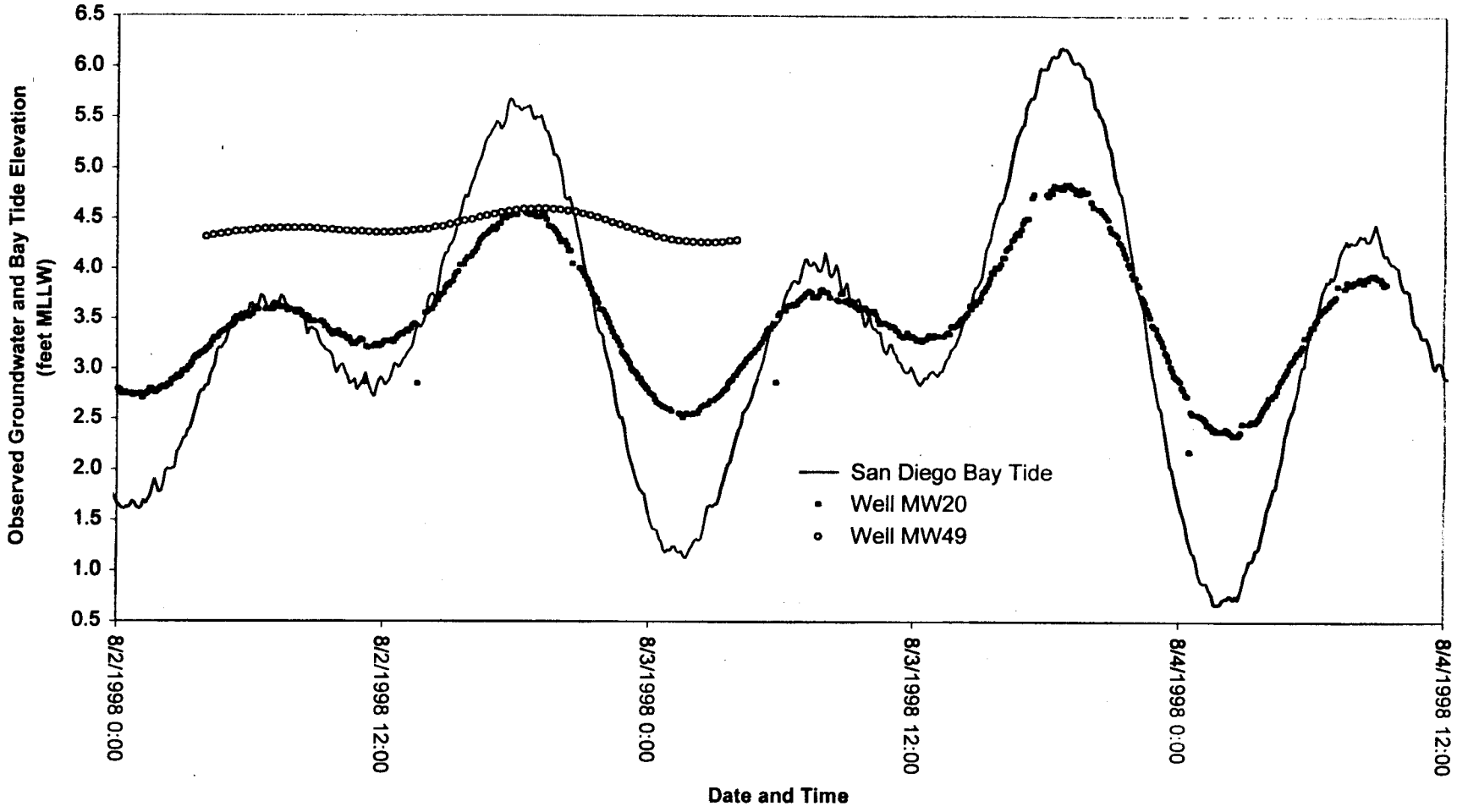


NAS NORTH ISLAND SITE 9
NoVOCs™ HYDROGEOLOGICAL INVESTIGATION

**FIGURE 5-7**
**OBSERVED WATER LEVEL COMPARISON AMONG BAY TIDE, MW20 AND MW49**

Tetra Tech EM Inc.

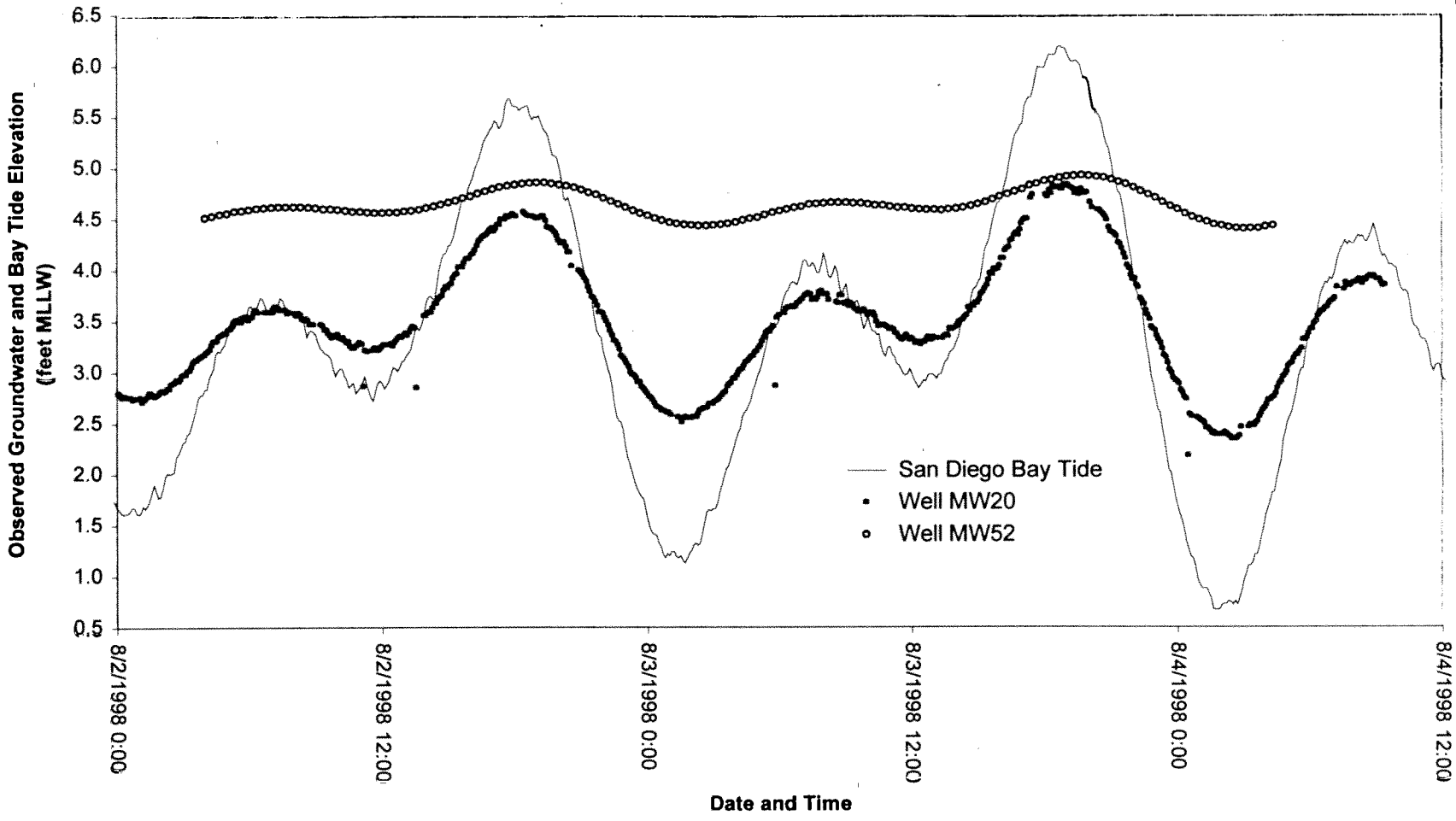


NAS NORTH ISLAND SITE 9
NoVOCs™ HYDROGEOLOGICAL INVESTIGATION

**FIGURE 5-8**
**OBSERVED WATER LEVEL COMPARISON AMONG BAY TIDE, MW20 AND MW52**

Tetra Tech EM Inc.

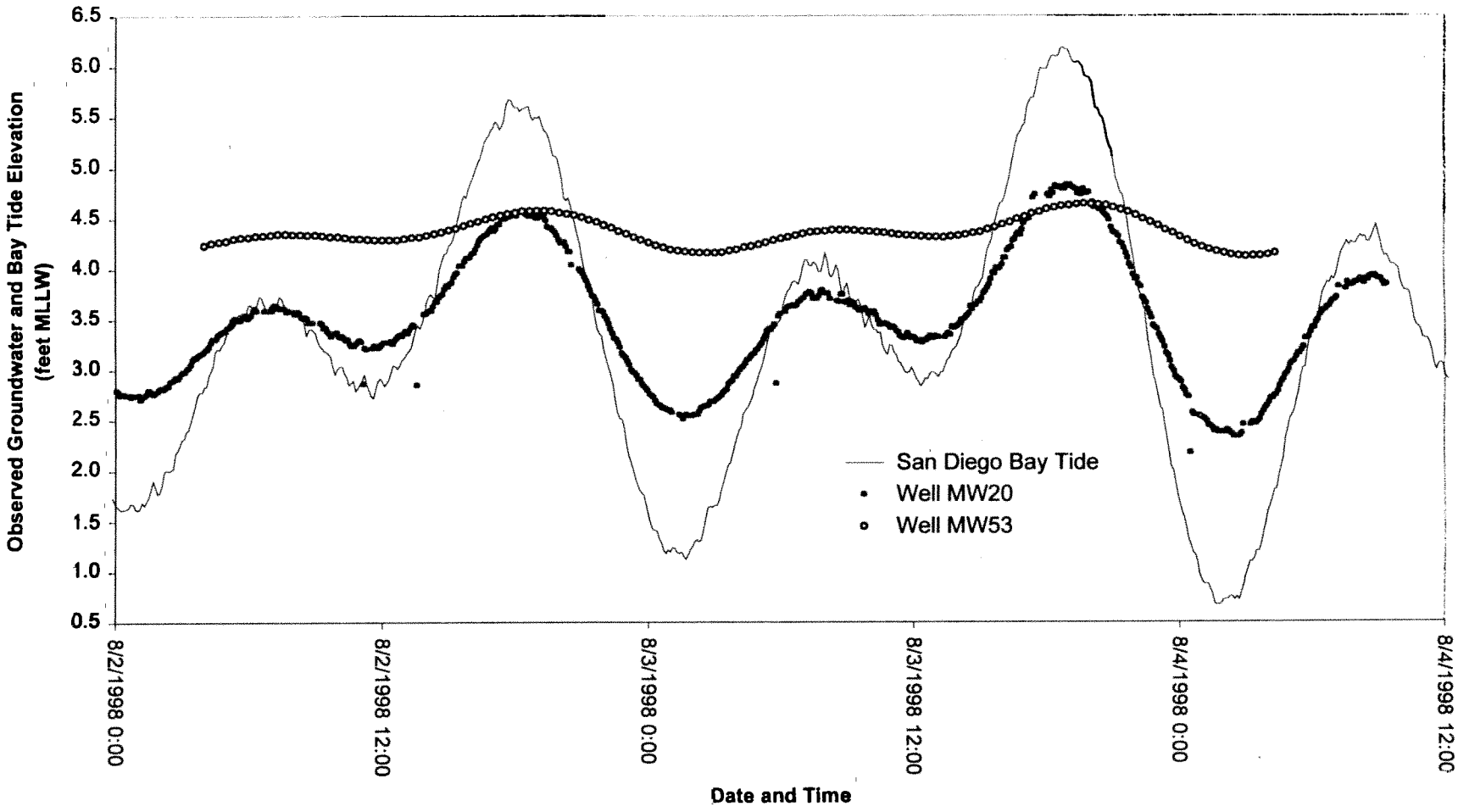


NAS NORTH ISLAND SITE 9
NoVOCs™ HYDROGEOLOGICAL INVESTIGATION

**FIGURE 5-9**
**OBSERVED WATER LEVEL COMPARISON AMONG BAY TIDE, MW20 AND MW53**

Tetra Tech EM Inc.

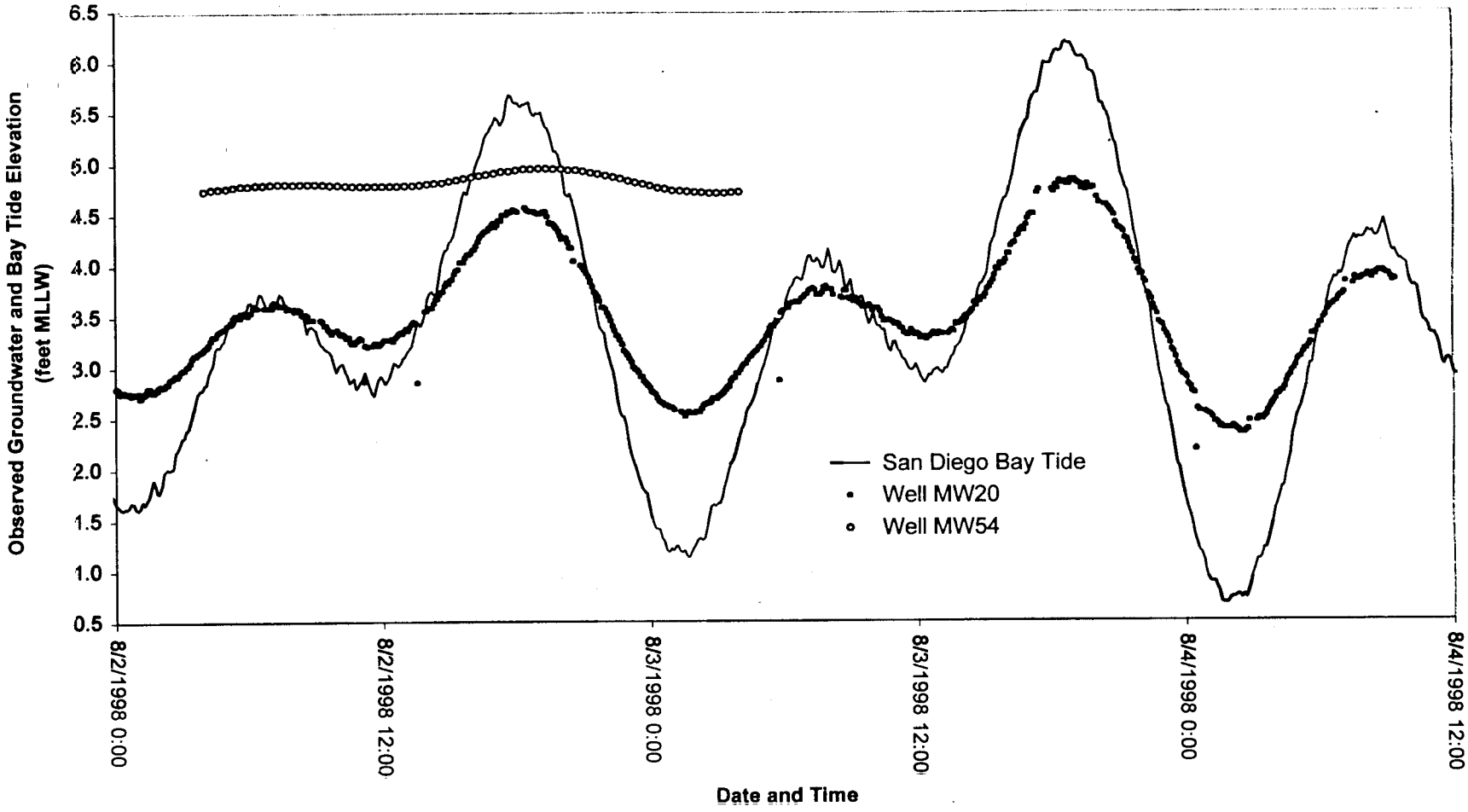


NAS NORTH ISLAND SITE 9
NoVOCs™ HYDROGEOLOGICAL INVESTIGATION

**FIGURE 5-10**
**OBSERVED WATER LEVEL COMPARISON AMONG BAY TIDE, MW20 AND MW54**

Tetra Tech EM Inc.

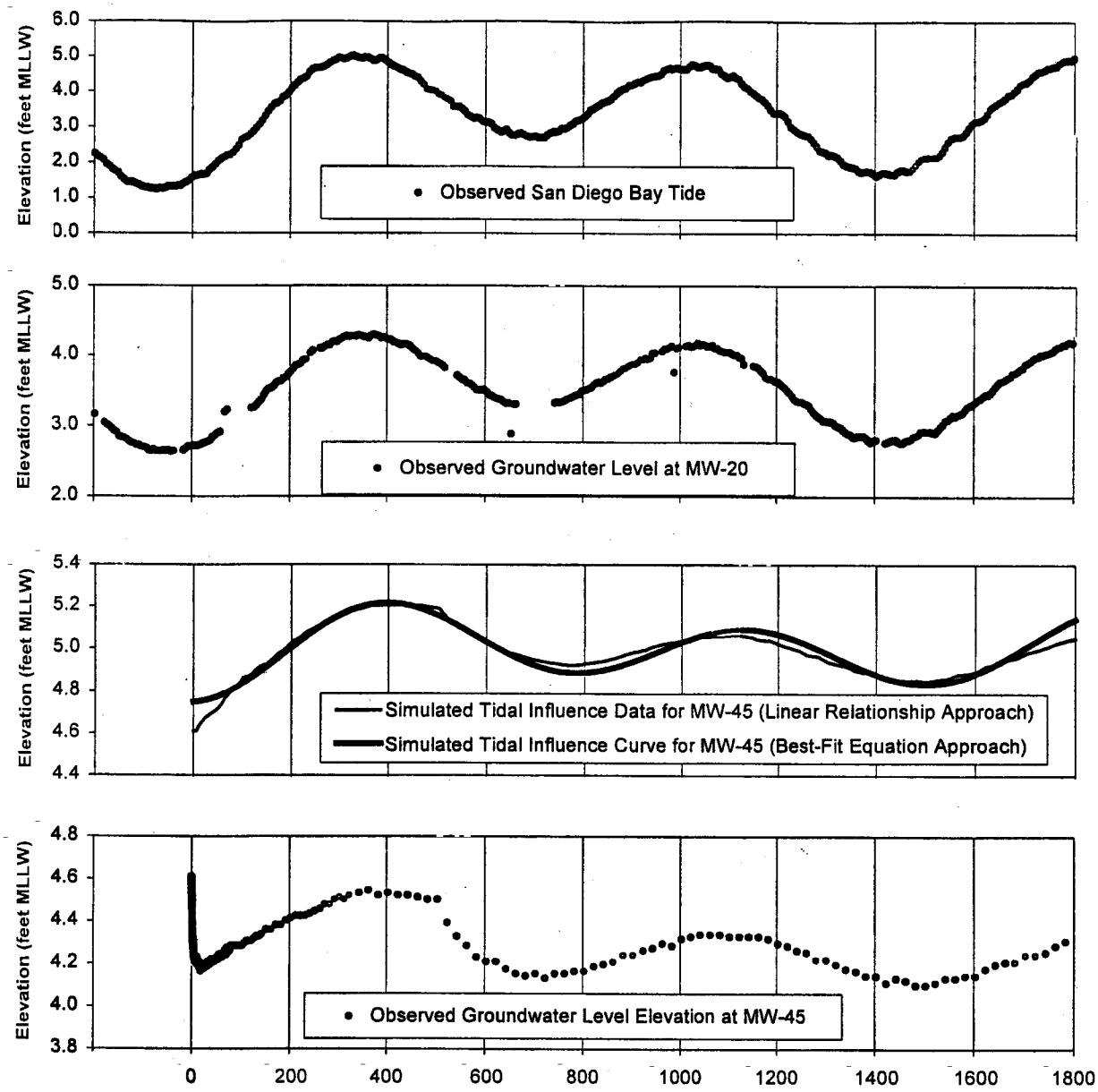


NAS NORTH ISLAND SITE 9
NoVOCs™ HYDROGEOLOGICAL INVESTIGATION

**FIGURE 5-11**
**OBSERVED AND SIMULATED WATER LEVEL COMPARISON AMONG BAY TIDE, MW20, MW45 DURING THE PUMPING TEST**
(Upper Aquifer Zone Constant Rate Pumping Test)

Tetra Tech EM Inc.

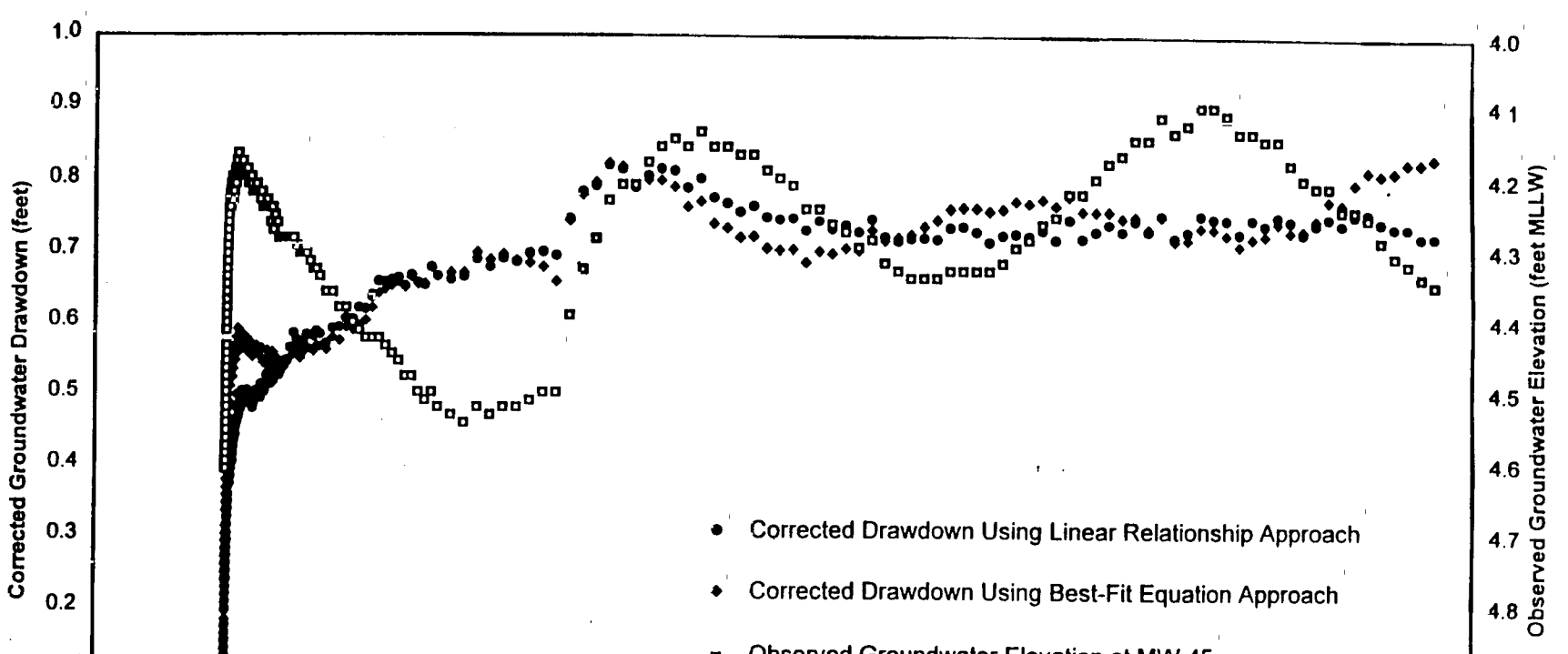


NAS NORTH ISLAND SITE 9
NoVOCs™ HYDROGEOLOGICAL INVESTIGATION

**FIGURE 5-12**
**OBSERVED AND CORRECTED GROUNDWATER DRAWDOWN AT WELL MW45**
(Upper Aquifer Zone Constant Rate Pumping Test)

Tetra Tech EM Inc.

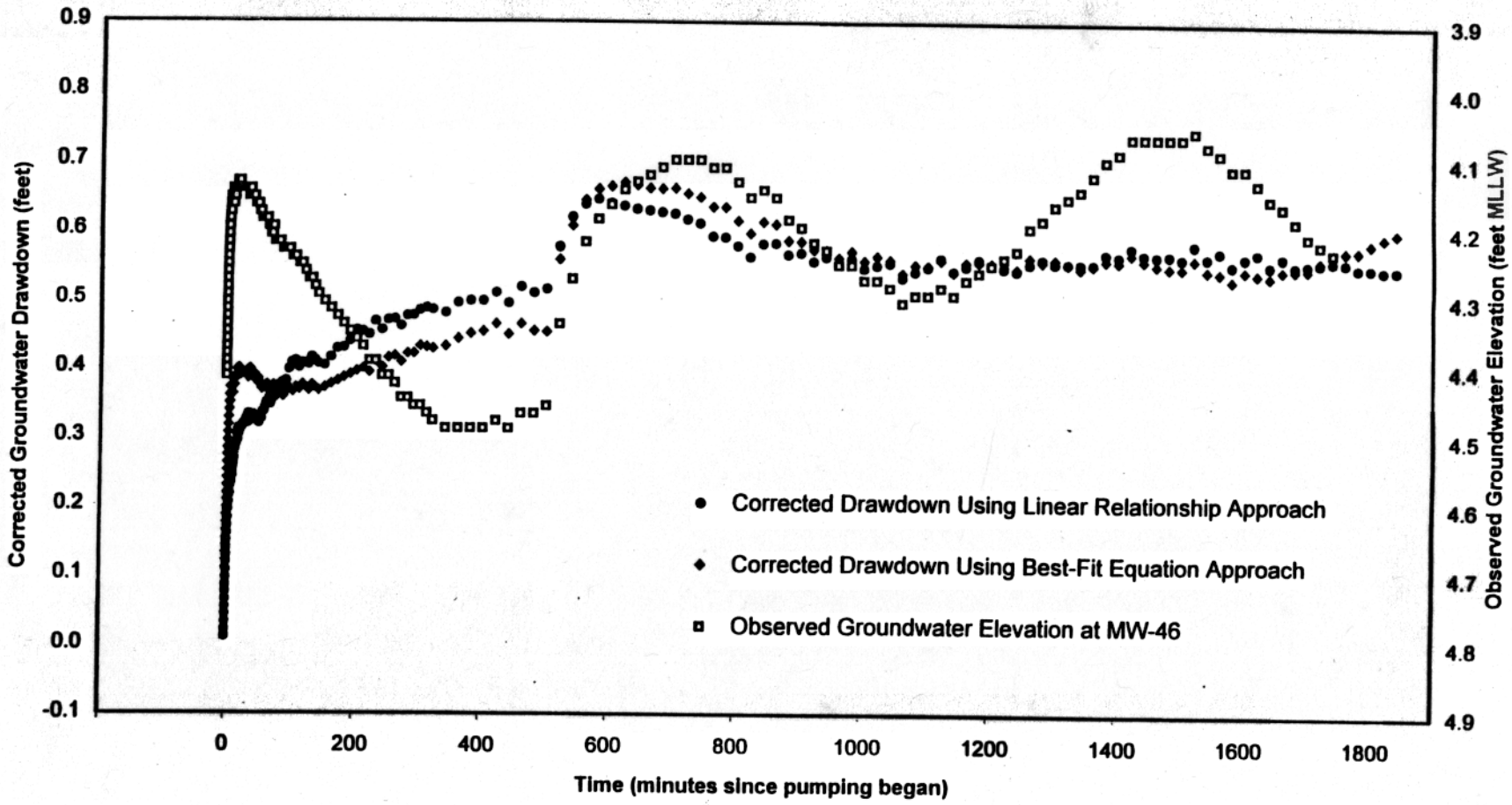


NAS NORTH ISLAND SITE 9
NoVOCs™ HYDROGEOLOGICAL INVESTIGATION

**FIGURE 5-13**
**OBSERVED AND CORRECTED GROUNDWATER DRAWDOWN AT WELL MW46**
(Upper Aquifer Zone Constant Rate Pumping Test)

Tetra Tech EM Inc.

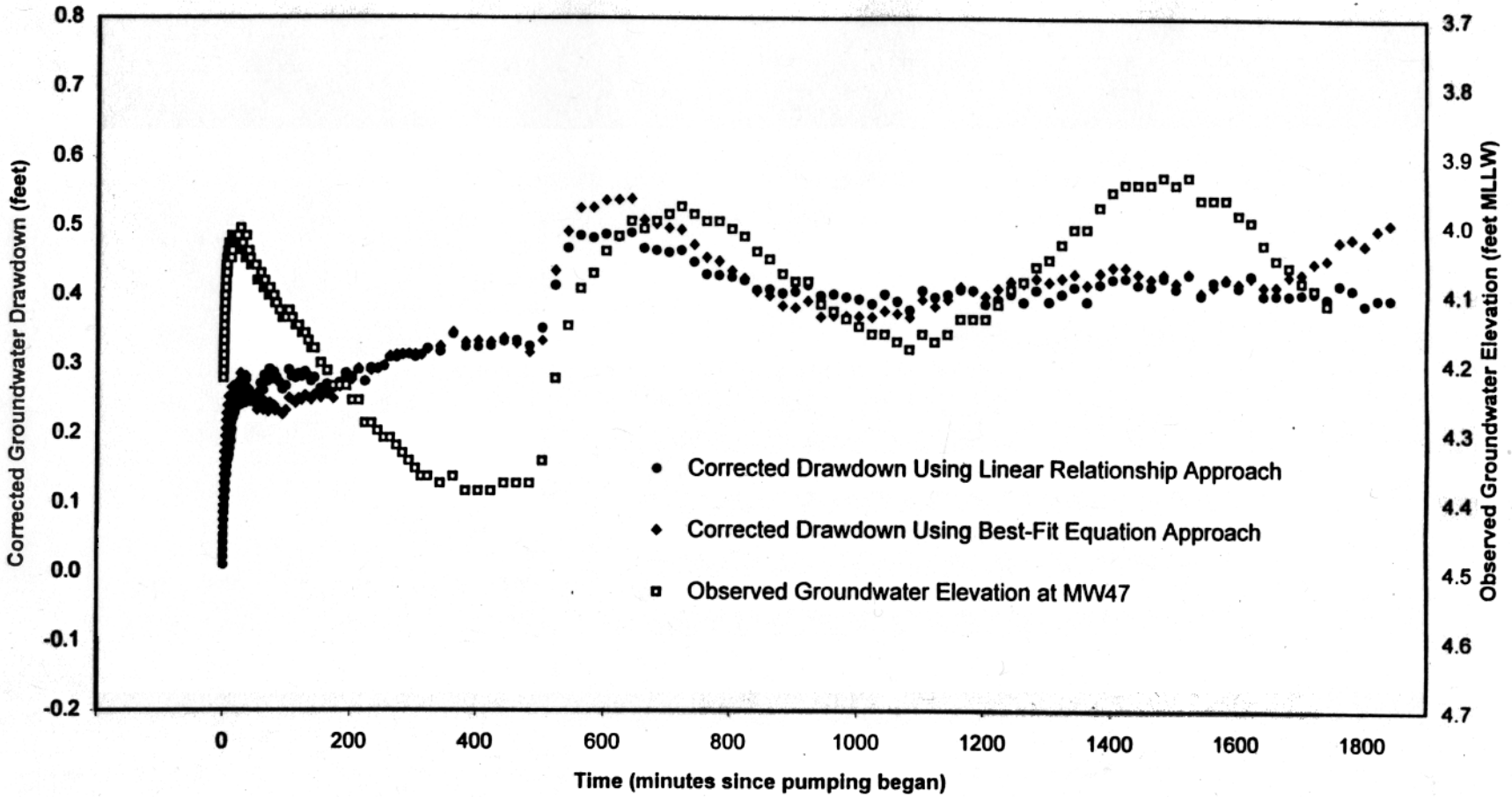


NAS NORTH ISLAND SITE 9
NoVOCs™ HYDROGEOLOGICAL INVESTIGATION

**FIGURE 5-14**
**OBSERVED AND CORRECTED GROUNDWATER DRAWDOWN AT WELL MW47**
(Upper Aquifer Zone Constant Rate Pumping Test)

Tetra Tech EM Inc.

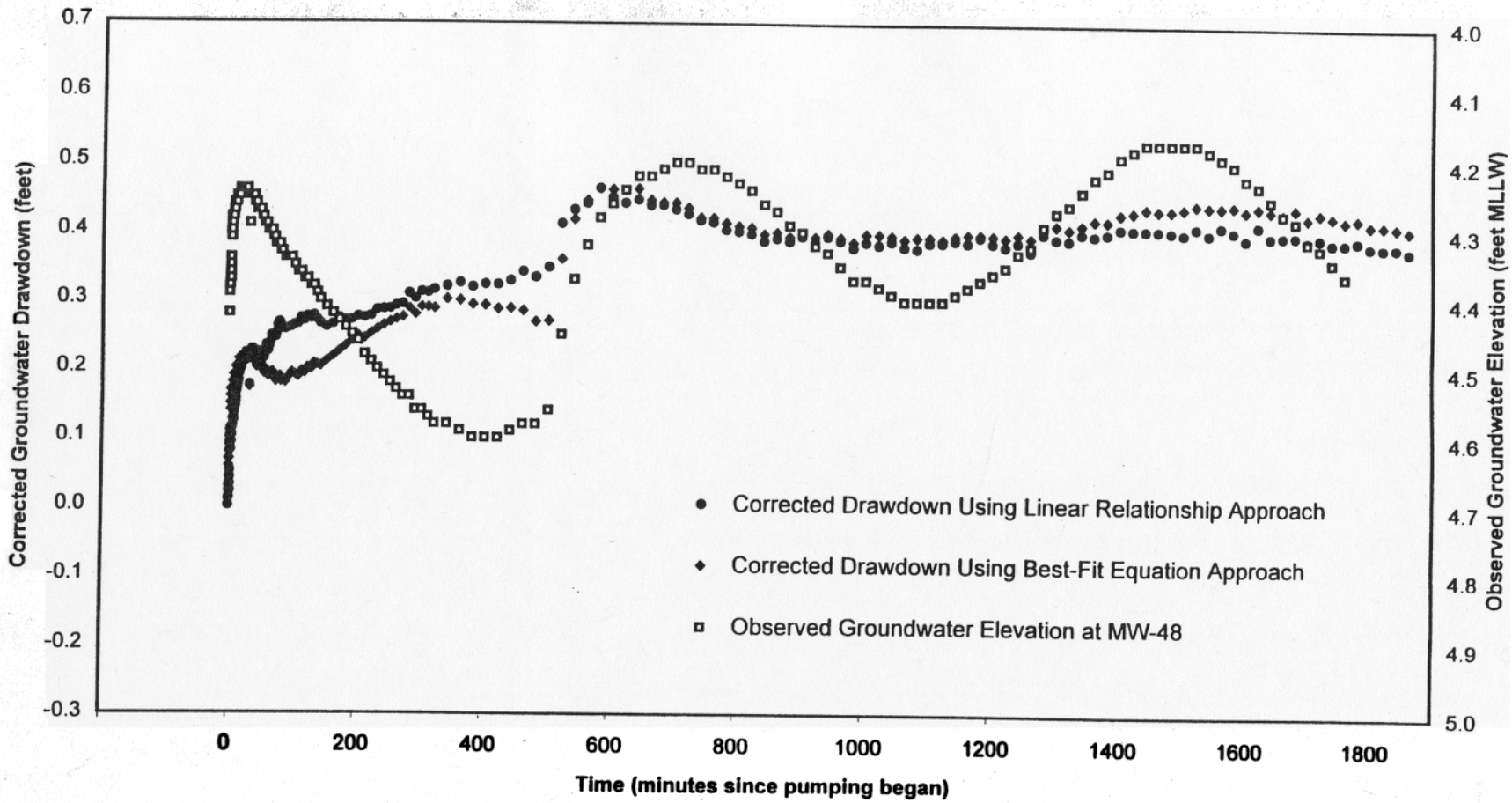


**NAS NORTH ISLAND SITE 9**
**NoVOCs™ HYDROGEOLOGICAL INVESTIGATION**

**FIGURE 5-15**
**OBSERVED AND CORRECTED GROUNDWATER DRAWDOWN AT WELL MW48**
(Upper Aquifer Zone Constant Rate Pumping Test)

Tetra Tech EM Inc.

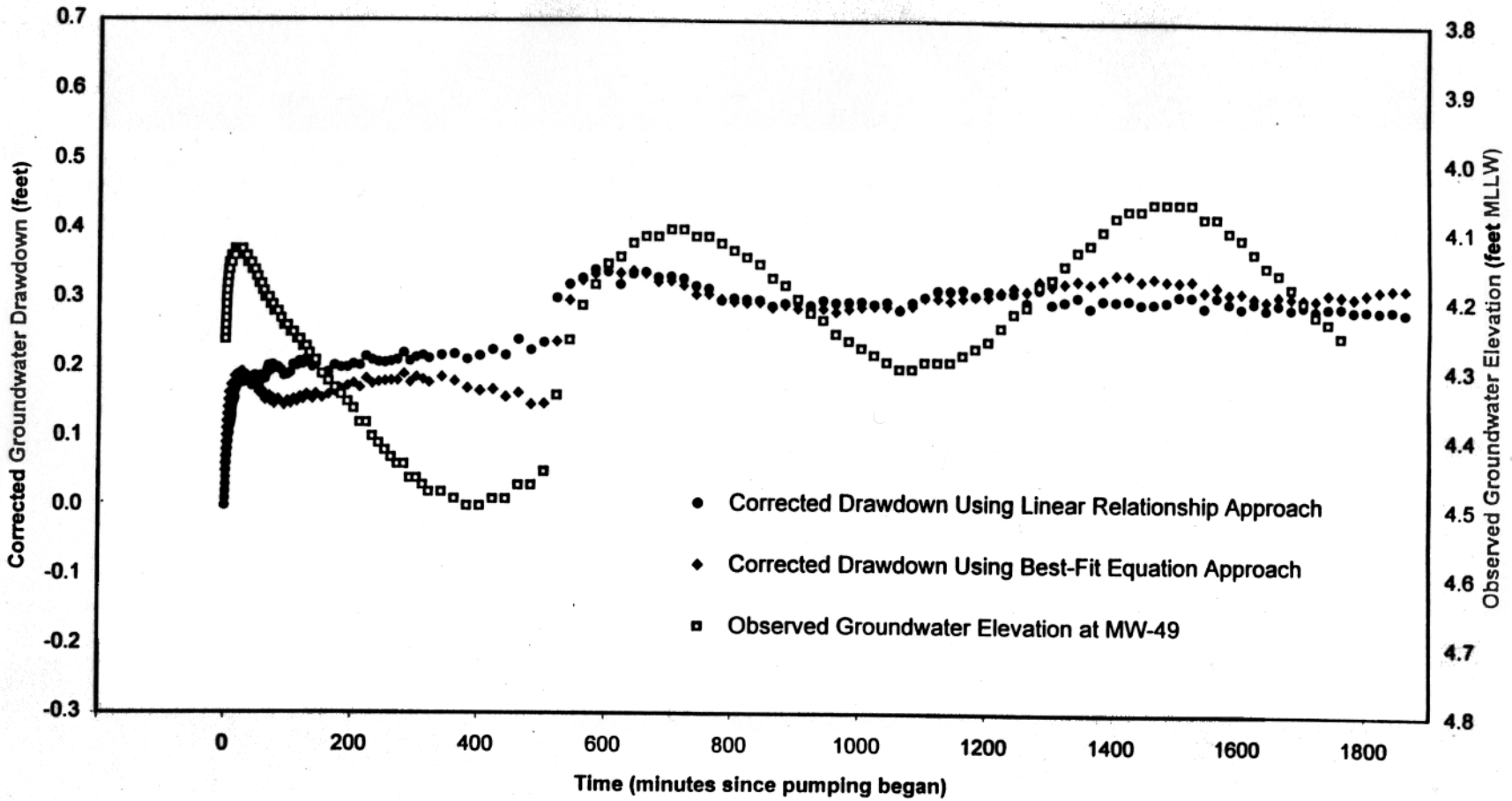


NAS NORTH ISLAND SITE 9
NoVOCs™ HYDROGEOLOGICAL INVESTIGATION

**FIGURE 5-16**
**OBSERVED AND CORRECTED GROUNDWATER DRAWDOWN AT WELL MW49**
(Upper Aquifer Zone Constant Rate Pumping Test)

Tetra Tech EM Inc.

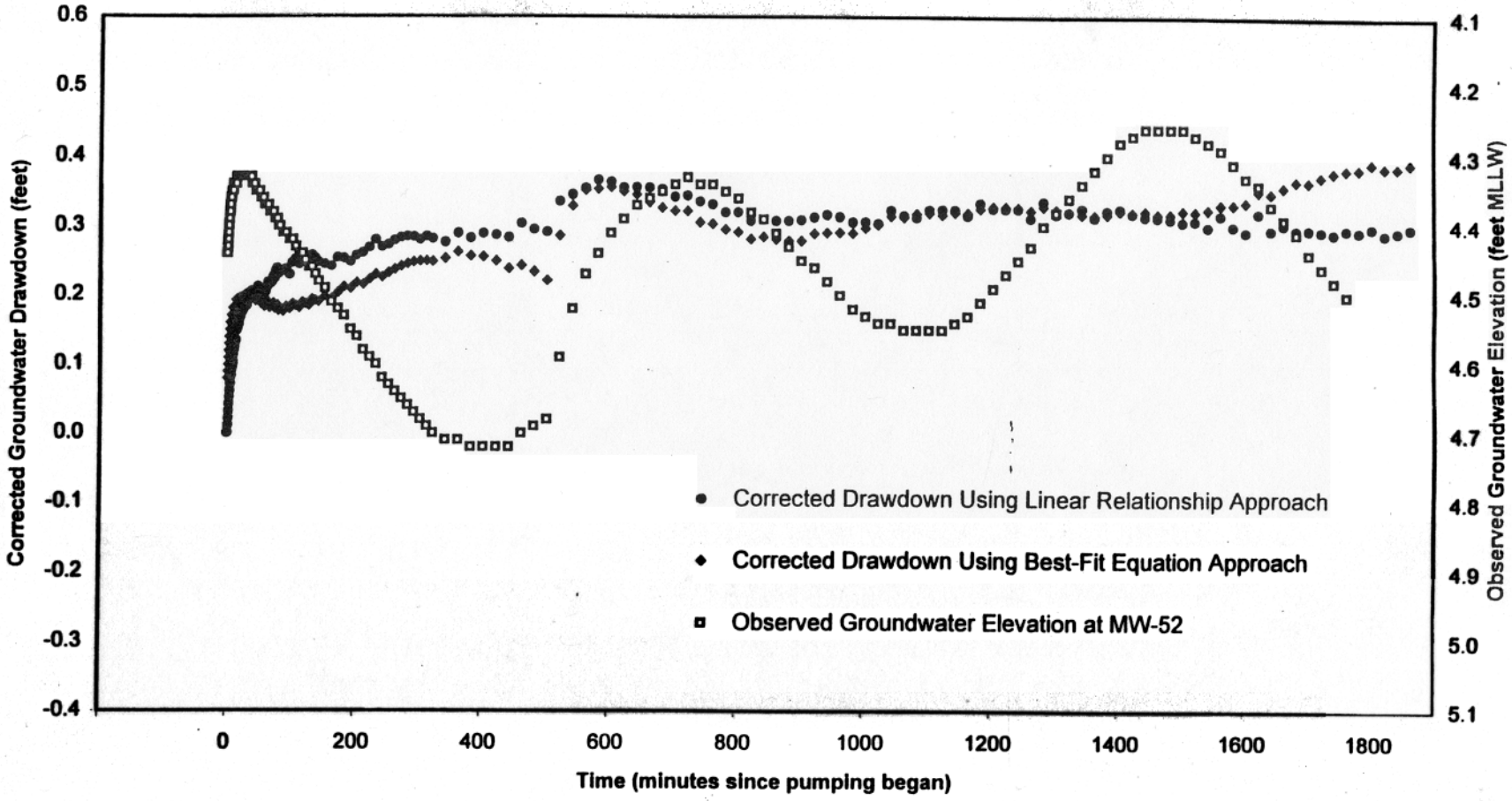


NAS NORTH ISLAND SITE 9
NoVOCs™ HYDROGEOLOGICAL INVESTIGATION

**FIGURE 5-17**
**OBSERVED AND CORRECTED GROUNDWATER DRAWDOWN AT WELL MW52**
(Upper Aquifer Zone Constant Rate Pumping Test)

Tetra Tech EM Inc.

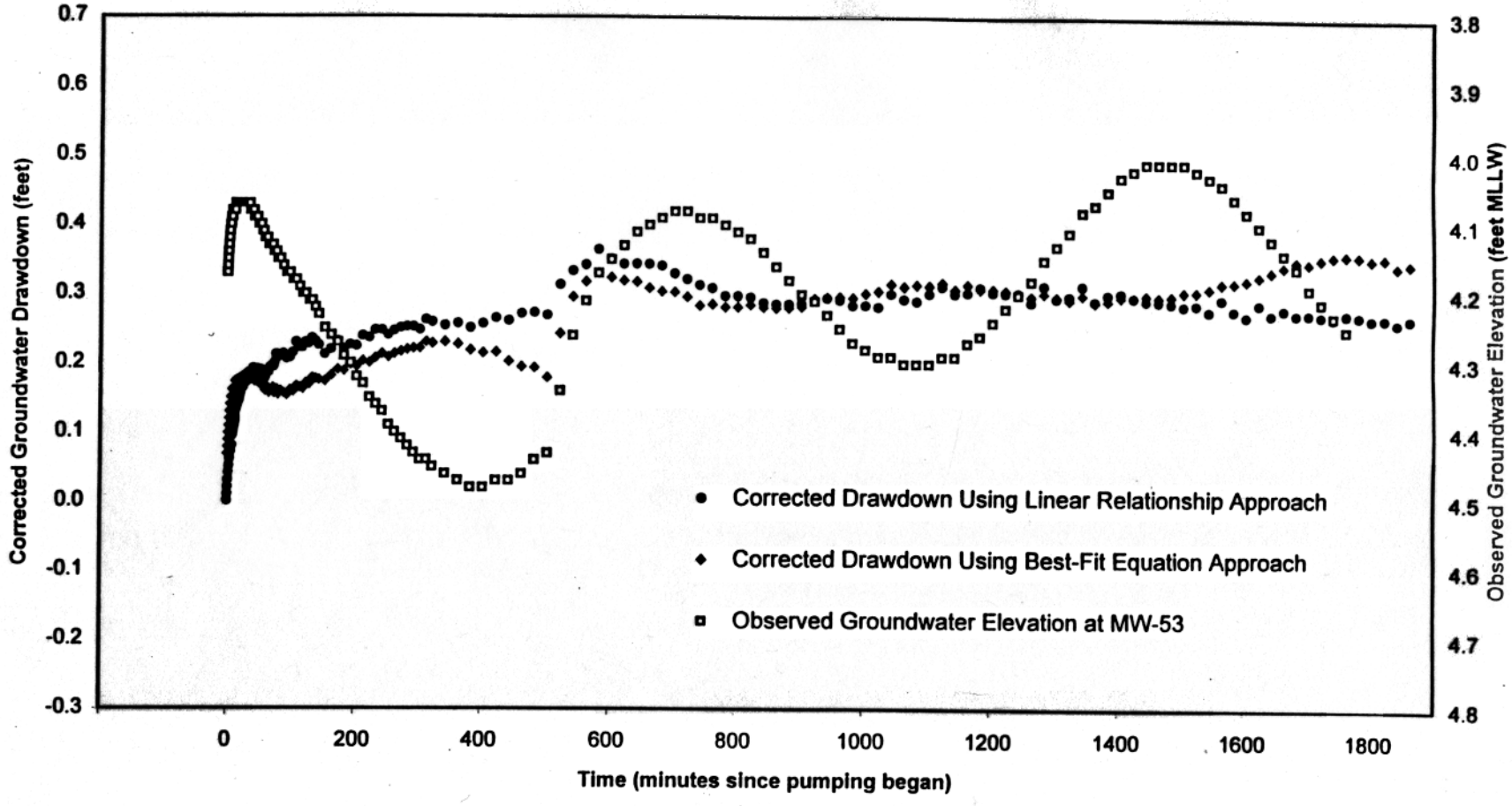


NAS NORTH ISLAND SITE 9
NoVOCs™ HYDROGEOLOGICAL INVESTIGATION

**FIGURE 5-18**
**OBSERVED AND CORRECTED GROUNDWATER DRAWDOWN AT WELL MW53**
(Upper Aquifer Zone Constant Rate Pumping Test)

Tetra Tech EM Inc.

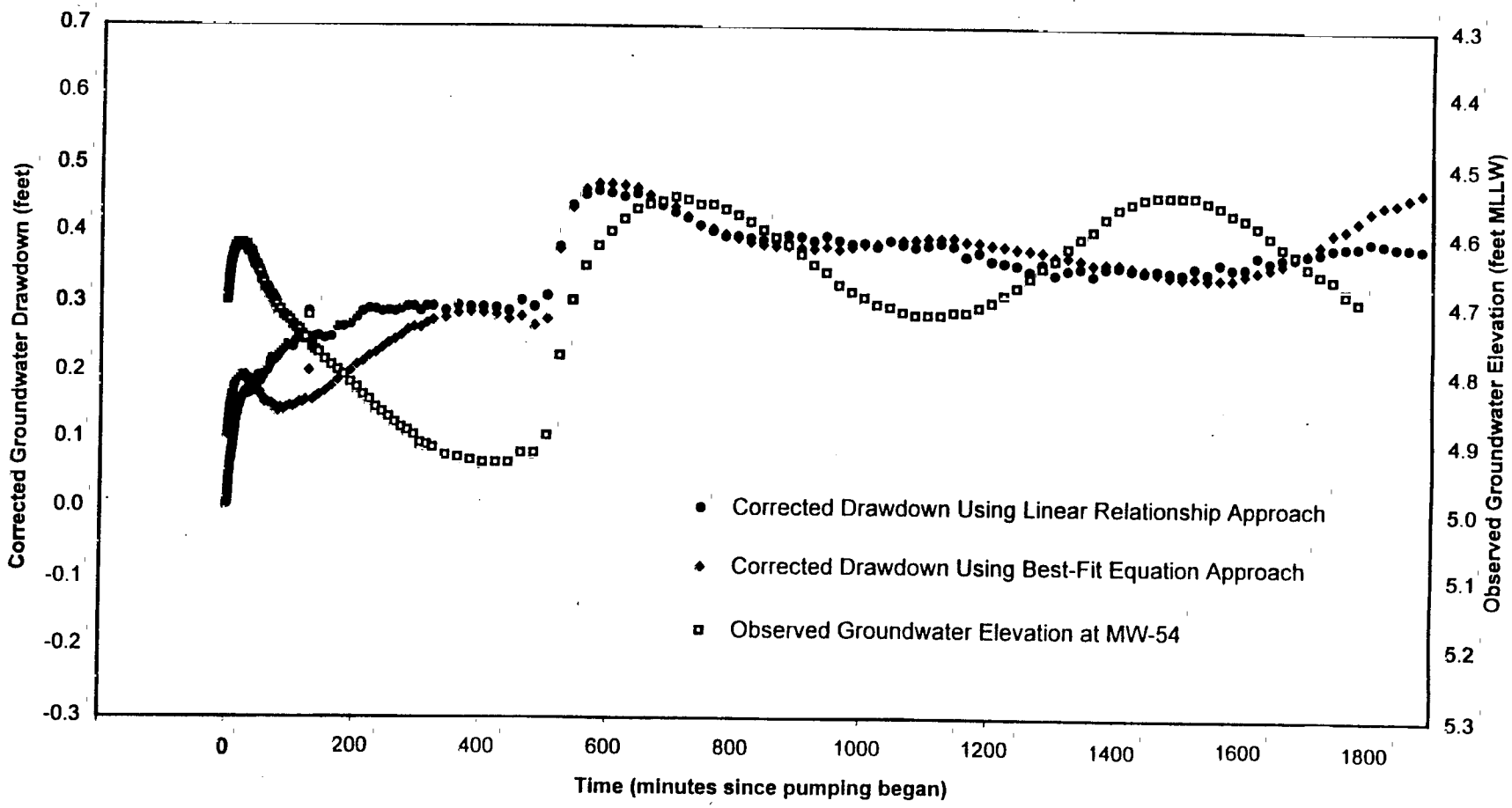


NAS NORTH ISLAND SITE 9
NoVOCs™ HYDROGEOLOGICAL INVESTIGATION

**FIGURE 5-19**
**OBSERVED AND CORRECTED GROUNDWATER DRAWDOWN AT WELL MW54**
(Upper Aquifer Zone Constant Rate Pumping Test)

Tetra Tech EM Inc.